Heat transfer in polyatomic gases

Behnam Rahimi and Henning Struchtrup

Citation: AIP Conference Proceedings **1786**, 070006 (2016); doi: 10.1063/1.4967582
View online: http://dx.doi.org/10.1063/1.4967582
View Table of Contents: http://scitation.aip.org/content/aip/proceeding/aipcp/1786?ver=pdfcov
Published by the AIP Publishing

Heat Transfer in Polyatomic Gases

Behnam Rahimi[1,a)] and Henning Struchtrup[1,b)]

[1]*Dept. of Mechanical Engineering, University of Victoria, Victoria, BC, Canada*

[a)]Corresponding author: behnamr@uvic.ca
[b)]struchtr@uvic.ca

Abstract. A high-order macroscopic model for the accurate description of rarefied polyatomic gas flows is used to explore heat transfer in rarefied polyatomic gases. The unsteady heat conduction of a gas at rest is studied numerically and analytically. The full boundary conditions are obtained for the macroscopic models of the refined Navier-Stokes-Fourier (RNSF) equations and the R19 equations. The results for different gases are given and effects of Knudsen numbers, degrees of freedom and temperature dependent properties are investigated. For some cases, the higher order effects are very dominant and the widely used first order set of the Navier-Stokes-Fourier equations fails to accurately capture the gas behavior and should be replaced by the proposed higher order set of equations.

INTRODUCTION

Recently, we introduced a sophisticated high order macroscopic model to describe rarefied polyatomic gases in transition regime [1, 2, 3, 4]. In the transition flow regime, the conventional hydrodynamics fails in the description of the gas behavior. The Boltzmann equation offers accurate description of the gas flow for all Kn numbers through modeling the evolution of velocity distribution function. However, solving the Boltzmann equation or related kinetic equation directly, deterministically or stochastically, is expensive and time consuming. As an alternative to the Boltzmann equation, kinetic theory provides macroscopic models for not too large Knudsen numbers, transition regime. Flows in micro-electro-mechanical systems (MEMS) and high vacuum systems are in this regime [5].

The Knudsen number, defined as the ratio of molecular mean free path to the characteristic length of the system $\left(Kn = \frac{\lambda}{L_0} = \frac{\tau}{\tau_0}\right)$, measures the degree of rarefaction of a gas flow. The exchange processes of colliding particles of a polyatomic gases could either exchange just translational (kinetic) energy or exchange both translational and internal energy which are characterized by the mean free times τ_{tr} and τ_{int}, respectively. Therefore, there are two distinct Knudsen numbers associated with above mean free times, Kn_{tr} and Kn_{int}.

In the present paper, we explore the stationary heat transfer in polyatomic gases. The results for different gases are given and effects of Knudsen numbers, degrees of freedom and temperature dependent properties are investigated. We lay out the formulation of the problem under consideration in the next section. Results are given and discussed in section 3 . Final conclusions are given in section 4.

PROBLEM FORMULATION

One dimensional heat transfer within the stationary polyatomic gas is studied. The sophisticated high order set of R19 equations is solved numerically and analytically along with the corresponding obtained boundary conditions. Also, the set of first order refined NSF equations are solved and compared with the R19 results. We consider an unsteady heat conduction which is homogeneous in y and z directions. The gas is confined between two infinite plates and is stationary, as shown in Figure 1. The walls are at different temperatures and the flow properties and variables depend only on x-direction. We study different gases and different test case scenarios.

The set of nondimensionalized R19 equations describing the problem under consideration is as follows:

30th International Symposium on Rarefied Gas Dynamics
AIP Conf. Proc. 1786, 070006-1–070006-8; doi: 10.1063/1.4967582
Published by AIP Publishing. 978-0-7354-1448-8/$30.00

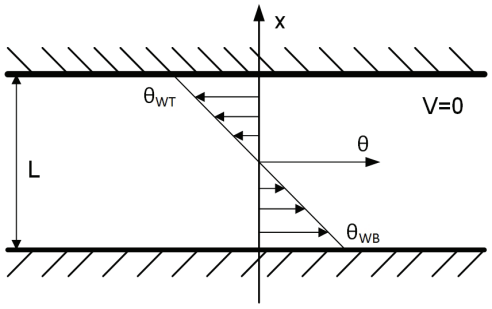

FIGURE 1. General stationary heat conduction schematic. Top and bottom walls are at different temperatures.

energy and momentum conservations and the balance laws for dynamic temperature $\Delta\theta$, stress tensor σ_{ij},

$$\frac{\partial\rho}{\partial x}+\frac{\partial\left(\theta-\Delta\theta\right)}{\partial x}+\frac{\partial\sigma_{11}}{\partial x}=0\,, \tag{1}$$

$$\frac{3+\delta+(1+\theta)\frac{d\delta}{d\theta}}{2}(1+\rho)\frac{\partial\theta}{\partial t}+\frac{\partial q}{\partial x}=0\,, \tag{2}$$

$$(1+\rho)\frac{\partial\Delta\theta}{\partial t}+\left(\frac{2}{3+\delta+(1+\theta)\frac{d\delta}{d\theta}}-\frac{10R_{q_{int}}}{3\left(5R_{q_{int}}+\left(\delta+(1+\theta)\frac{d\delta}{d\theta}\right)R_{q_{tr}}\right)}\right)\frac{\partial q}{\partial x}$$
$$-\frac{2\left(\delta+(1+\theta)\frac{d\delta}{d\theta}\right)R_{q_{tr}}}{3\left(5R_{q_{int}}+\left(\delta+(1+\theta)\frac{d\delta}{d\theta}\right)R_{q_{tr}}\right)}\frac{\partial\Delta q}{\partial x}+\frac{10R_{q_{int}}R_{q_{tr}}\left(2\frac{d\delta}{d\theta}+(1+\theta)\frac{d^2\delta}{d\theta^2}\right)}{3\left(5R_{q_{int}}+\left(\delta+(1+\theta)\frac{d\delta}{d\theta}\right)R_{q_{tr}}\right)^2}(q-\Delta q)\frac{\partial\theta}{\partial x}=-\frac{(1+\rho)}{\tau_{int}}\Delta\theta\,, \tag{3}$$

$$\frac{\partial\sigma_{11}}{\partial t}+\frac{2}{3}\frac{4R_{q_{int}}}{5R_{q_{int}}+\left(\delta+(1+\theta)\frac{d\delta}{d\theta}\right)R_{q_{tr}}}\frac{\partial q}{\partial x}+\frac{2}{3}\frac{4\left(\delta+(1+\theta)\frac{d\delta}{d\theta}\right)R_{q_{tr}}}{5\left(5R_{q_{int}}+\left(\delta+(1+\theta)\frac{d\delta}{d\theta}\right)R_{q_{tr}}\right)}\frac{\partial\Delta q}{\partial x}$$
$$+\frac{2}{3}\frac{4R_{q_{int}}R_{q_{tr}}\left(2\frac{d\delta}{d\theta}+(1+\theta)\frac{d^2\delta}{d\theta^2}\right)}{\left(5R_{q_{int}}+\left(\delta+(1+\theta)\frac{d\delta}{d\theta}\right)R_{q_{tr}}\right)^2}(\Delta q-q)\frac{\partial\theta}{\partial x}+\frac{\partial u^{0,0}_{111}}{\partial x}=-\left[\frac{1}{\tau_{tr}}+\frac{1}{\tau_{int}}\right]\sigma_{11}\,, \tag{4}$$

overall heat flux q, heat flux difference Δq,

$$\frac{\partial q}{\partial t}+\left(1+\theta+\Delta\theta-\frac{1}{\rho}\sigma_{11}\right)\frac{\partial\sigma_{11}}{\partial x}+\frac{5+\delta+(1+\theta)\frac{d\delta}{d\theta}}{2}\left[(1+\rho)\left[1+\theta-\Delta\theta\right]+\sigma_{11}\right]\frac{\partial\theta}{\partial x}+\frac{168}{(42+25\delta)^2}B^{+}_{11}\frac{d\delta}{d\theta}\frac{\partial\theta}{\partial x}$$
$$-\frac{2}{39}\frac{\partial B^{+}}{\partial x}+\frac{5}{13}\frac{\partial B^{-}}{\partial x}+\frac{7\left(3+\delta\right)\left(14+3\delta\right)}{\left(14+\delta\right)\left(42+25\delta\right)}\frac{\partial B^{-}_{11}}{\partial x}+\left[\sigma_{11}-(1+\rho)\left[1+\theta+\Delta\theta\right]\right]\frac{\partial\Delta\theta}{\partial x}$$
$$+\frac{4\delta}{(42+25\delta)}\frac{\partial B^{+}_{11}}{\partial x}-\left[\frac{(1+\theta-\Delta\theta)\,\sigma_{11}}{(1+\rho)}+\Delta\theta^2\right]\frac{\partial\rho}{\partial x}+7\left(\frac{1}{(14+\delta)^2}-\frac{24}{(42+25\delta)^2}\right)B^{-}_{11}\frac{d\delta}{d\theta}\frac{\partial\theta}{\partial x}$$
$$=-\left[\frac{1}{\tau_{tr}}+\frac{1}{\tau_{int}}\right]\left(\frac{R_{q_{int}}R_{q_{tr}}\left(5+\delta+(1+\theta)\frac{d\delta}{d\theta}\right)}{5R_{q_{int}}+\left(\delta+(1+\theta)\frac{d\delta}{d\theta}\right)R_{q_{tr}}}q+\frac{\left(\delta+(1+\theta)\frac{d\delta}{d\theta}\right)R_{q_{tr}}\left(R_{q_{tr}}-R_{q_{int}}\right)}{5R_{q_{int}}+\left(\delta+(1+\theta)\frac{d\delta}{d\theta}\right)R_{q_{tr}}}\Delta q\right)\,, \tag{5}$$

$$\frac{\partial \Delta q}{\partial t}+\left[\sigma_{11}-\frac{5}{2}\left(1+\frac{3R_{q_{int}}}{\left(\delta+(1+\theta)\frac{d\delta}{d\theta}\right)R_{q_{tr}}}\right)(1+\rho)(1+\theta+\Delta\theta)\right]\frac{\partial \Delta\theta}{\partial x}-\frac{5}{39}\left(1+\frac{3R_{q_{int}}}{\left(\delta+(1+\theta)\frac{d\delta}{d\theta}\right)R_{q_{tr}}}\right)\frac{\partial B^{+}}{\partial x}$$
$$+\left[\frac{(\Delta\theta-1-\theta)}{1+\rho}\sigma_{11}-\frac{5}{2}\left(1+\frac{3R_{q_{int}}}{\left(\delta+(1+\theta)\frac{d\delta}{d\theta}\right)R_{q_{tr}}}\right)\Delta\theta^{2}\right]\frac{\partial \rho}{\partial x}+\left[1+\theta+\frac{5}{2}\left(1+\frac{3R_{q_{int}}}{R_{q_{tr}}\left(\delta+(1+\theta)\frac{d\delta}{d\theta}\right)}\right)\Delta\theta\right]\frac{\partial \sigma_{11}}{\partial x}$$
$$+\frac{5}{39}\left(1-\frac{10R_{q_{int}}}{\left(\delta+(1+\theta)\frac{d\delta}{d\theta}\right)R_{q_{tr}}}\right)\frac{\partial B^{-}}{\partial x}+\frac{\delta}{(42+25\delta)}\left(7+\frac{15R_{q_{int}}}{\left(\delta+(1+\theta)\frac{d\delta}{d\theta}\right)R_{q_{tr}}}\right)\frac{\partial B^{+}_{11}}{\partial x}$$
$$+\left(\frac{5}{2}\left[1-\frac{R_{q_{int}}}{R_{q_{tr}}}\right][\sigma_{11}+(1+\rho)(1+\theta+\Delta\theta)]+\frac{42\left(7+\frac{15R_{q_{int}}}{\left(\delta+(1+\theta)\frac{d\delta}{d\theta}\right)R_{q_{tr}}}\right)}{(42+25\delta)^{2}}\frac{d\delta}{d\theta}B^{+}_{11}\right)\frac{\partial \theta}{\partial x}$$
$$=-\left[\frac{1}{\tau_{tr}}+\frac{1}{\tau_{int}}\right]\left(\frac{5R_{q_{int}}\left(R_{q_{tr}}-R_{q_{int}}\right)}{5R_{q_{int}}+\left(\delta+(1+\theta)\frac{d\delta}{d\theta}\right)R_{q_{tr}}}q+\frac{\left(\delta+(1+\theta)\frac{d\delta}{d\theta}\right)R^{2}_{q_{tr}}+5R^{2}_{q_{int}}}{5R_{q_{int}}+\left(\delta+(1+\theta)\frac{d\delta}{d\theta}\right)R_{q_{tr}}}\Delta q\right), \quad (6)$$

equations for higher moments B^{+} and B^{-}, and the constitutive equations for the higher moments B^{+}_{ij}, B^{-}_{ij} and $u^{0,0}_{ijk}$, which are not shown here due to lack of space. Note that the dimensionless relaxation times , τ_{int} and τ_{tr}, are the Knudsen numbers.

The corresponding first order equations, refined Navier Stokes Fourier (RNSF), to the stationary heat conduction problem under consideration are,

$$\frac{\partial \rho}{\partial x}+\frac{\partial \theta}{\partial x}=0\,, \quad (7a)$$
$$\frac{3+\delta+(1+\theta)\frac{d\delta}{d\theta}}{2}(1+\rho)\frac{\partial \theta}{\partial t}+\frac{\partial q}{\partial x}=0\,, \quad (7b)$$
$$q=-\tau_{tr}\frac{5R_{q_{int}}+\left(\delta+(1+\theta)\frac{d\delta}{d\theta}\right)R_{q_{tr}}}{2R_{q_{int}}R_{q_{tr}}}(1+\rho)(1+\theta)\frac{\partial \theta}{\partial x}\,. \quad (7c)$$

Where, the stress tensor and dynamic temperature are obtained to be zero at this order, for the problem under consideration.

Steady linearized set of equations with small disturbances from an equilibrium ground state $\{\rho_0, v^0_i=0, \theta_0\}$ are reduced to 5 coupled equations for $\Phi=\{\Delta q,\ q,\ u^{0,0}_{111},\ \sigma_{11},\ \Delta\theta\}$ and the rest of the variables $\{\rho,\ \theta,\ B^{+},\ B^{-}\}$ are functions of them. The solution of set of coupled equations, $A_{5\times5}\frac{\partial \Phi}{\partial x}=B_{5\times5}\Phi$, is obtained using the eigenvalue method.

The finite difference method is used to discretize our system of equations with second order accuracy in spatial discretization and first order discretization in time.

BOUNDARY CONDITIONS

The microscopic boundary condition introduced in Ref.[1] is used to obtain macroscopic boundary conditions. We obtained for wall density,

$$\rho_w\sqrt{\theta_w}=-\frac{(14-\delta)(3+\delta)}{2(14+\delta)(42+25\delta)\theta^{\frac{3}{2}}}B^{-}_{11}+\frac{1}{156}\frac{B^{+}-B^{-}}{\theta^{\frac{3}{2}}}-\frac{\delta}{2(42+25\delta)\theta^{\frac{3}{2}}}B^{+}_{11}+\frac{1}{2}\frac{\sigma_{11}}{\sqrt{\theta}}+\frac{1}{2\sqrt{\theta}}\rho(2\theta-\Delta\theta)=\Upsilon\,. \quad (8)$$

Nondimensionalized boundary condition for total heat flux is obtained as,

$$q=-n_y\frac{\chi}{(2-\chi)}\sqrt{\frac{2}{\pi(1+\theta)}}\left[\frac{(56-\delta(1-\zeta))}{312}B^{-}+(3+\delta)\frac{(140+\delta(32+\delta)+(14-\delta)\delta\zeta)}{4(14+\delta)(42+25\delta)}B^{-}_{11}\right.$$
$$+\frac{[(1-\zeta)\delta-4]}{312}B^{+}+\frac{\delta(4-\delta(1-\zeta))}{4(42+25\delta)}B^{+}_{11}-\frac{(2+\delta(1-\zeta))}{4}(1+\theta)((1+\rho)\Delta\theta-\sigma_{11})$$
$$\left.+\frac{\delta(1-\zeta)}{2}(1+\rho)(1+\theta)^{2}+\frac{\Upsilon}{2}\sqrt{(1+\theta)}[(4+\delta\zeta)(\theta-\theta_w)-(1-\zeta)(\delta(1+\theta)+3\Delta\theta)]\right], \quad (9)$$

nondimensionalized boundary condition for heat flux difference and for $u^{0,0}_{yyy}$ are obtained as,

$$\Delta q = n_y \frac{\chi}{(2-\chi)\,\mathrm{Pr}_{q_{tr}}\left(\delta+(1+\theta)\frac{d\delta}{d\theta}\right)}\sqrt{\frac{2}{\pi(1+\theta)}}\Bigg[\frac{5(6-\delta)\,\mathrm{Pr}_{q_{int}}+12\left(\delta+(1+\theta)\frac{d\delta}{d\theta}\right)\mathrm{Pr}_{q_{tr}}}{4}(1+\rho)(1+\theta)\Delta\theta$$
$$+\frac{5(12+\delta)\,\mathrm{Pr}_{q_{int}}+12\left(\delta+(1+\theta)\frac{d\delta}{d\theta}\right)\mathrm{Pr}_{q_{tr}}}{312}B^{+}-\delta\frac{5(6+\delta)\,\mathrm{Pr}_{q_{int}}+6\left(\delta+(1+\theta)\frac{d\delta}{d\theta}\right)\mathrm{Pr}_{q_{tr}}}{4(42+25\delta)}B^{+}_{11}$$
$$+[3+\delta]\frac{5\delta(42+\delta)\,\mathrm{Pr}_{q_{int}}-6(14-\delta)\left(\delta+(1+\theta)\frac{d\delta}{d\theta}\right)\mathrm{Pr}_{q_{tr}}}{4(14+\delta)(42+25\delta)}B^{-}_{11}+\frac{5(40-\delta)\,\mathrm{Pr}_{q_{int}}-12\left(\delta+(1+\theta)\frac{d\delta}{d\theta}\right)\mathrm{Pr}_{q_{tr}}}{312}B^{-}$$
$$+\frac{10\delta\,\mathrm{Pr}_{q_{int}}-8\left(\delta+(1+\theta)\frac{d\delta}{d\theta}\right)\mathrm{Pr}_{q_{tr}}}{4}(1+\rho)(1+\theta)^2+\frac{5\delta\,\mathrm{Pr}_{q_{int}}-6\left(\delta+(1+\theta)\frac{d\delta}{d\theta}\right)\mathrm{Pr}_{q_{tr}}}{4}(1+\theta)\sigma_{yy}+\frac{\Upsilon}{2}\sqrt{(1+\theta)}$$
$$\left[-15\underset{q_{int}}{\mathrm{Pr}}(1-\zeta)\Delta\theta-\left(5\delta\underset{q_{int}}{\mathrm{Pr}}-4\left(\delta+(1+\theta)\frac{d\delta}{d\theta}\right)\underset{q_{tr}}{\mathrm{Pr}}\right)(1+\theta)+\left(5\delta\zeta\underset{q_{int}}{\mathrm{Pr}}-4\left(\delta+(1+\theta)\frac{d\delta}{d\theta}\right)\underset{q_{tr}}{\mathrm{Pr}}\right)(\theta-\theta_W)\right]\Bigg], \quad (10)$$

$$u^{0,0}_{111} = n_y\frac{\chi\sqrt{\frac{2}{\pi(1+\theta)}}}{(2-\chi)}\Bigg[\frac{(-14+\delta)(3+\delta)B^{-}_{11}}{(14+\delta)(42+25\delta)}-\frac{\delta B^{+}_{11}}{42+25\delta}-\frac{2(B^{+}-B^{-})}{195}$$
$$-\frac{7\sigma_{11}+2(1+\rho)\Delta\theta}{5}(1+\theta)+\Upsilon\frac{2}{5}\sqrt{(1+\theta)}[\theta-\theta_W]\Bigg]. \quad (11)$$

These boundary conditions have to hold on both walls with $n_y = \pm 1$ for lower and upper wall, respectively. Last boundary condition is the prescribe mass condition, $\int_{-\frac{1}{2}}^{\frac{1}{2}}\rho dx = 0$.

RESULTS

We first compare the results of our proposed models with the Direct Simulation Monte Carlo method data [6]. Comparison between numerical solution of the R19, the RNSF equations and DSMC results are shown in Figure 2. Dimensionless wall temperatures are at ±0.0476 and reference temperature at 350 K. We investigate two different reference Kn numbers, 0.071 and 0.71, which represent slip and transition flow regimes, respectively. The relaxation parameters are set to $R_{u^{2,0}} = R_{q_{tr}} = 0.7$ and $R_{q_{int}} = R_{u^{1,1}} = 0.736$. Therefore, we have the Prandtl number,

$$\mathrm{Pr} = \frac{\left(5+\delta+\theta\frac{d\delta}{d\theta}\right)R_{q_{int}}R_{q_{tr}}}{5R_{q_{int}}+\left(\delta+\theta\frac{d\delta}{d\theta}\right)R_{q_{tr}}}, \quad (12)$$

equals to 0.73 same as DSMC simulation of Ref. [6]. Also, excited internal degrees of freedom is set to 2. It is evident from Figure 2 that there is a good agreement between the DSMC and the R19 results. However in transition regime, there is a considerable deviation of Refined Navier–Stokes–Fourier equations results from DSMC results and first order set of equations fails to accurately model the problem.

The developing profiles from equilibrium ground state initial condition $\{\rho_0, \theta_0\}$ to steady state condition are presented for H_2 gas in Figure 3. Prandtl number is set to 0.69, reference temperature is at 300 K and dimensionless wall temperatures are ±0.5. The shear viscosity temperature exponent is set to 0.5. Reference time scale is set to be equal to reference internal time scale, $\tau_0 = \tau_{int}$, and we have

$$\begin{cases} Kn_{tr} = 0.0091 \\ Kn_{int} = 1 \end{cases}. \quad (13)$$

The results presented in Figure 3 are obtained from numerical solution of R19 set of equations with the initial conditions of the reference equilibrium state $\{\rho_0, \theta_0\}$. It is depicted that total temperature and density is rising from zero starting from regions near walls and gradually in time moving towards central region. Other variables start from zero

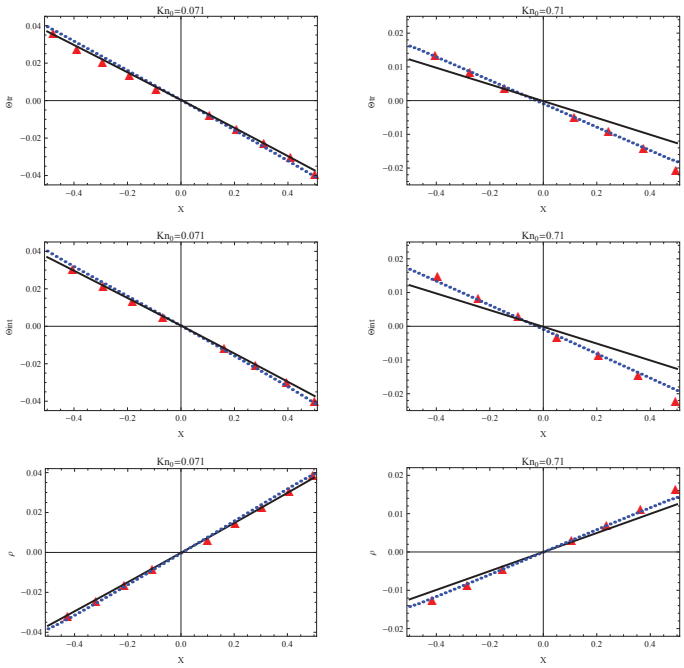

FIGURE 2. Comparison of temperature and density profiles for Kn numbers equal to 0.071 and 0.71. Results shown are obtained from: set of R19 equations, blue dashed; set of RNSF equations, black line; DSMC method, red triangles.

at initial state and jump to their maximum value first of all as the boundary feels the temperature jump and then start to decay over time to reach their steady state profiles as the boundary effects reach the middle section. The speed of these decays are not constant and their values keep reducing in time. The values of nonequilibrium variables at the beginning of the process are order of magnitude higher than their values in steady state.

The effects of different range of temperatures are studied on N_2 gas in Figure 4. We investigate two cases with upper dimensionless wall temperature at 0.5 and 2.5. The lower wall temperature and reference temperature are kept fixed at 300 K and referenced Kn numbers are fixed at $Kn_{tr} = 0.077$ and $Kn_{int} = 0.2$ for two cases under study. As it can be seen, the main effect here is promoting the non-symmetry effects by the temperature dependent properties and relaxation times in the case with higher upper wall temperature.

Now, we compare three different gases with distinguished characteristics, H_2, N_2 and CH_4, in Figure 5. Reference and wall's temperatures are fixed at 700 K, 0 and 0.5, respectively. Translational Knudsen number is also kept fixed at 0.032. The corresponding reference Kn_{int} are obtained to be

$$Kn_{int} = \begin{cases} N_2: & 0.158 \\ H_2: & 3.78 \\ CH_4: & 10 \end{cases} . \tag{14}$$

Number of excited internal degrees of freedom at reference temperature of these gases are

$$\delta + \theta \frac{d\delta}{d\theta} = \begin{cases} N_2: & 2.41 \\ H_2: & 2.09 \\ CH_4: & 8.89 \end{cases} . \tag{15}$$

H_2 and CH_4 gases both have large differences between internal and translational relaxation times. However, internal and translational relaxation times of N_2 gas have comparable values. On the other hand, H_2 and N_2 gases both have similar excited internal degrees of freedom. Nonetheless, excited internal DoF of CH_4 gas is higher than the other two gases. The effects of having internal and translational relaxation times at the same order are seen in profiles of moments corresponding to deviations from total values, $\Delta\theta$ and Δq, which are derived by translational-internal

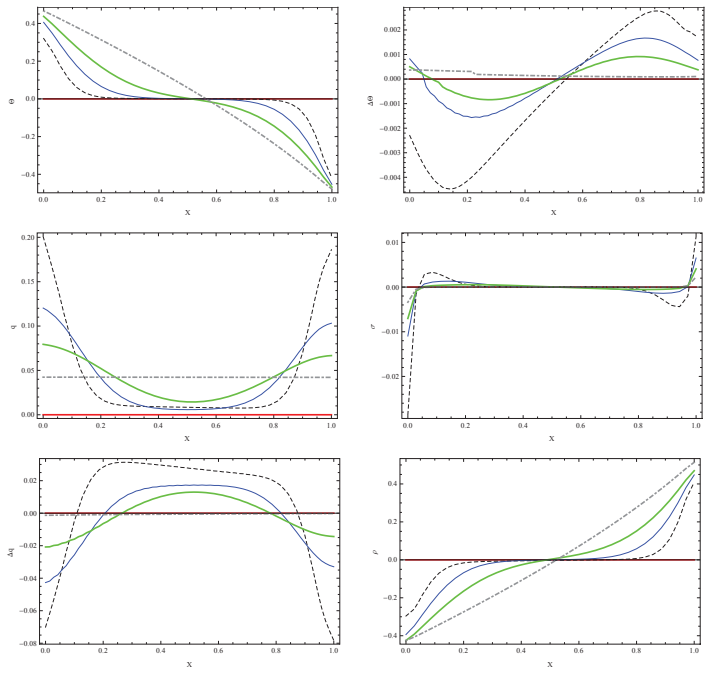

FIGURE 3. Numerical results of stationary heat conduction from set of R19 equations. Red line is at $t = 0$ s; black-dashed is at $t = 0.2$ s; blue-thin line is at t=0.6 s; green-thick is at $t = 1.5$ s; gray-dotdashed is at $t = 29$ s.

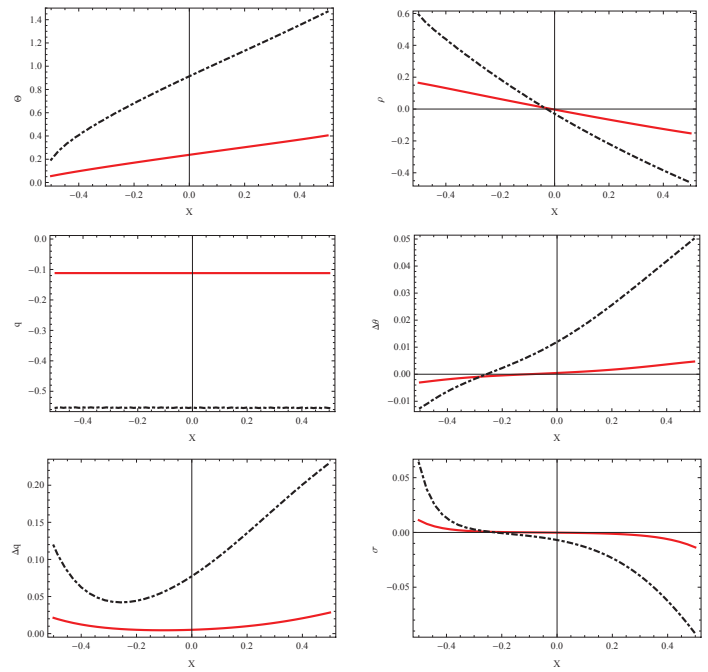

FIGURE 4. Steady state profiles of N_2 gas obtained from numerical method with $\theta_{WB} = 0$ and Red line: $\theta_{WT} = 0.5$; black-dotdashed: $\theta_{WT} = 2.5$.

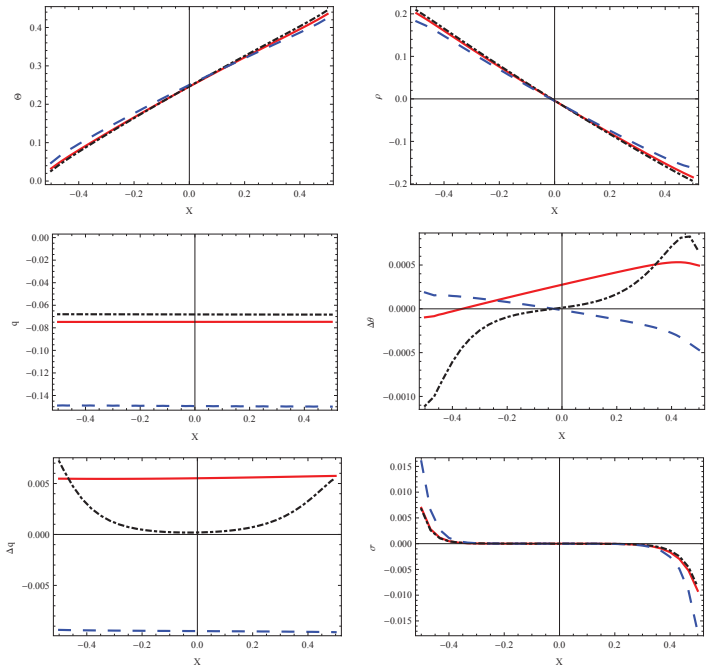

FIGURE 5. Steady state profiles of different gases obtained from numerical solution of the R19 equations. Red line: H_2; black-dotdashed: N_2; blue-dashed: CH_4.

interactions. These effects are towards promoting the temperature dependency of the profiles, which now covers a larger range of values between two walls. The cases with higher internal Kn number has higher temperature jump and velocity slip. Due to the lower internal relaxation times and more active internal exchange processes in N_2 case, value of dynamic temperature is slightly higher compare to H_2 case. Also, less active internal exchange processes produced higher heat fluxes. This strong effects of different ratios of Kn numbers are diminished at low translational Knudsen number. The effects of different internal DoF are most seen in total heat flux and stress tensor. CH_4 gas with higher DoF gains higher total heat flux and stress tensor in comparison with other two gases. Also, the dynamic temperature, which is a nonequilibrium variable illustrating internal-translational exchanges are increased with increasing internal degrees of freedom. Increasing the internal degrees of freedom, slightly increases the temperature jump by increasing normal heat flux and dynamic temperature.

Effects of the reference temperature on variables is studied in Figure 6. N_2 gas with fixed reference translational Knudsen number at 0.077 and dimensionless wall temperatures at 0 and 0.5 is used with different reference temperatures of 300 and 700 K. The corresponding reference internal Knudsen numbers are 0.2 and 0.38, respectively. As it is depicted in Figure 6, the case with higher reference temperature, which means more excited internal degrees of freedom, have higher heat flux value and more flatter deviation moments, $\Delta\theta$ and Δq, profiles in comparison with lower reference temperature. Also, there is slightly higher temperature jump, especially on bottom wall, in case of higher reference temperature in comparison with the lower one case.

CONCLUSIONS

We solved unsteady one-dimensional stationary heat conduction numerically and analytically with set of the R19 and RNSF equations and compared the results with DSMC simulations. It was shown that the Navier-Stokes-Fourier equations were not accurate in transition regime. The results from set of R19 equations was in a good agreement with DSMC simulations. The values of nonequilibrium variables at the beginning of the unsteady process found to be an order of magnitude higher than their values in steady state. Effects of non-linearity and temperature dependent properties were more dominant in profiles associated with translational-internal variables ($\Delta\theta$ and Δq). The impor-

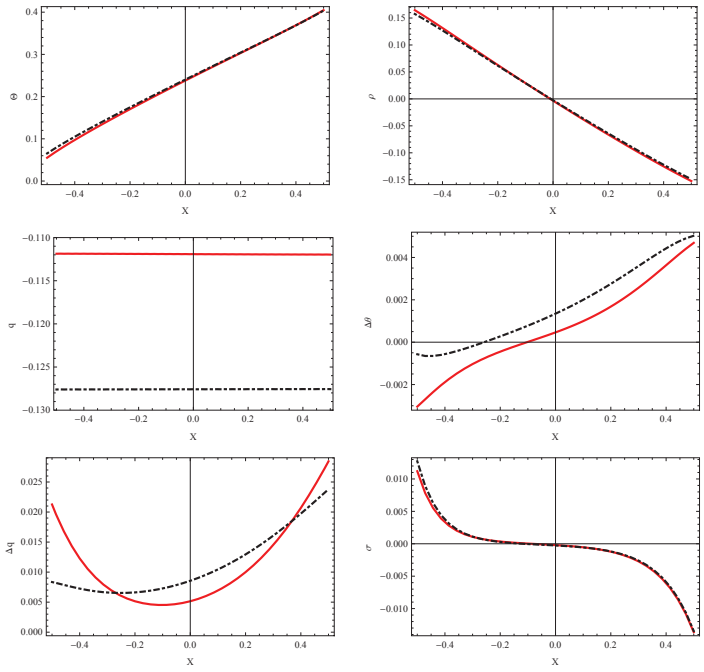

FIGURE 6. Steady state profiles of N_2 gas obtained from numerical method of the R19 equations with $\theta_{WB} = 0$ and $\theta_{WT} = 0.5$. Red line: $T_0 = 300$; black-dotdashed: $T_0 = 700$.

tance of our proposed model with the capability to model temperature dependent properties was shown in problems with relatively high temperature variations. The effects of having internal and translational relaxation times at the same order found to be on moments corresponding to deviations from total values, $\Delta\theta$ and Δq, which are derived by translational-internal interactions. These effects were towards promoting the temperature dependency effects and obtained profiles covered a larger range of values. The effects of different internal DoF were most seen in total heat flux and stress tensor, where gas with higher DoF gains higher total heat flux and stress tensor in comparison with gas with lower DoF. Higher reference temperature, which means more excited internal degrees of freedom, produced higher heat flux value and more flatter deviation moments, $\Delta\theta$ and Δq, profiles in comparison with lower reference temperature case.

ACKNOWLEDGMENTS

Support from the Natural Sciences and Engineering Research Council (NSERC) is gratefully acknowledged.

REFERENCES

[1] B. Rahimi and H. Struchtrup, (in press), Macroscopic and kinetic modeling of rarefied polyatomic gases, Journal of Fluid Mechanics **806** (2016).
[2] B. Rahimi and H. Struchtrup, AIP Conference Proceedings **1628**, 618–625 (2014).
[3] B. Rahimi and H. Struchtrup, Physics of Fluids **26** (2014), http://dx.doi.org/10.1063/1.4873577.
[4] B. Rahimi and H. Struchtrup, "Refined navier-stokes-fourier equations for rarefied polyatomic gases," in *ASME 2014 12th International Conference on Nanochannels, Microchannels, and Minichannels* (2014), pp. V001T01A001–V001T01A001.
[5] B. Rahimi and H. Niazmand, Heat Transfer Engineering **35**, 1528–1538 (2014).
[6] C. Tantos, D. Valougeorgis, and A. Frezzotti, International Journal of Heat and Mass Transfer **88**, 636 – 651 (2015).